Gravitational radiation – In celebration of Einstein's *Annus Mirabilis*

B. S. Sathyaprakash

School of Physics and Astronomy, Cardiff University, Cardiff, CF24 3YB, UK

Two of Einstein's 1905 papers were on special theory of relativity. Although general relativity was to come a decade later, it was special relativity that was responsible for the existence of wave-like phenomena in gravitation. A hundred years after the discovery of special relativity we are poised to detect gravitational waves and the detection might as well come from another inevitable and exotic prediction of relativity, namely black holes. With interferometric gravitational wave detectors taking data at unprecedented sensitivity levels and bandwidth, we are entering a new century in which our view of the Universe might be revolutionized yet again with the opening of the gravitational window. The current generation of interferometric and resonant mass detectors are only the beginning of a new era during which the gravitational window could be observed by deploying pulsar and microwave background radiation.

Keywords: *Annus Mirabilis*, gravitational radiation, gravitational waves.

1. Introduction

WE are celebrating 100 years of Einstein's *Annus Mirabilis* 1905, during which he published four papers on three subjects, thereby laying the foundation for quantum theory, the theory of Brownian motion, and the special theory of relativity. Each of these subjects has revolutionized our world view but the story is not over yet. Though it was not until 1915 that he founded the general theory of relativity, it was special relativity that is responsible for the existence of gravitational radiation. The waves have eluded direct detection so far but there is little doubt today about their existence thanks to spectacular observations of the decay in the orbital period of Galactic binary neutron stars[1,2].

Gravity is generated by the densities and currents of the energy and momentum of matter; if they change then the gravitational field changes. In Einstein's theory of gravity, unlike in Newtonian gravity, changes in the distribution of a source cannot travel instantaneously but at the speed of light. Indeed, the field equations of general relativity admit wave-like solutions that are in many ways similar to electromagnetic (EM) radiation but with important differences. Gravitational interaction is Universal and, although weak, gravity is non-linear. Universality of gravitation means that one cannot infer the influence of gravitational waves by watching an isolated particle in space, as opposed to EM radiation whose influence on a single charged particle can be inferred. One would need at least two particles, just as one would in Einstein's gedanken lift-experiment to infer the presence of the Earth's gravitational field. The weakness of the interaction means that on the one hand it will be very difficult to generate gravitational waves in the laboratory; only catastrophic astronomical events involving massive accelerations of bulk matter, as opposed to EM waves which are produced by accelerated charged particles, can produce significant amplitudes of the radiation. On the other hand the radiation carries the true signature of the emitting source, be it the core of a neutron star or a supernova, the quasi-normal mode oscillations of a black hole, or the birth of the Universe, thereby making it possible to observe phenomena and objects that are not directly accessible to the electromagnetic, neutrino or the cosmic-ray window. This is unlike EM waves which interact very strongly with matter and therefore imprint on the radiation from a source is the characteristic of its 'surface' rather than the core. Non-linearity of gravitational waves implies that the waves interact with the source resulting in a rich structure in the shape of the emitted signals that will be useful for testing relativity in new ways.

Gravitational radiation can be characterized by a dimensionless amplitude which is a measure of the deformation in space caused by the wave as it passes by. For instance, if two masses are initially separated by a distance ℓ, a wave of amplitude h causes a change in length $\delta\ell = h\ell/2$. Typical astronomical events, say a binary black hole merger at 100 Mpc, would have an amplitude $h \sim 10^{-23}$ at a frequency ~ 100 Hz, incurring a change in length of $\sim 10^{-20}$ m between masses separated by a distance $\ell \sim 1$ km. Detectors that are currently in operation will be able to observe such events which are expected to occur about once per year.

In the rest of this article we will discuss astronomical sources of gravitational waves. This article chiefly deals with compact objects, namely neutron stars (NS) and black holes (BH). Unless specified otherwise we shall assume that a NS has a mass of $M = 1.4M_\odot$ and radius $R = 10$ km, and by a stellar mass BH we shall mean a black hole of mass $M = 10M_\odot$. We shall assume a flat Universe with a cold dark matter density of $\Omega_M = 0.27$, dark energy of $\Omega_\Lambda = 0.70$, and a Hubble constant of $H_0 = 65$ km s^{-1} Mpc^{-1}. We shall use

e-mail: B.Sathyaprakash@astro.cf.ac.uk

a system of units in which $c = G = 1$, which means $1\ M_\odot \simeq 5 \times 10^{-6}$ s $\simeq 1.5$ km, 1 Mpc $\simeq 10^{14}$ s.

I will begin this article with a brief overview of gravitational wave (GW) theory and their interaction with matter and how that is used in the construction of detectors. The main focus of the article will be the astronomical sources of gravitational waves.

2. Gravitational wave theory – A brief overview

A key point of Newton's gravity is that because the potential satisfies Poisson equation, $\nabla^2\varphi(t, \mathbf{x}) = 4\pi\rho(t, \mathbf{x})$, there are no retardation effects. Since there are no time-derivatives involved on the LHS and the same time t appears both on the LHS and the RHS, any change in the distribution of density at the location of the source would instantaneously change the potential at the remote field point. In Einstein's theory the metric components of the background spacetime are the gravitational potentials and they satisfy a wave equation and hence there will be retardation effects. This is explicitly seen in the linearized version of Einstein's equations.

Under the assumption of weak gravitational fields one can assume that the background metric $g_{\alpha\beta}$ of spacetime to be only slightly different from the Minkowski metric $\eta_{\alpha\beta} = \mathrm{Diag}(-1, 1, 1, 1) : g_{\alpha\beta} = \eta_{\alpha\beta} + h_{\alpha\beta}$, $|h_{\alpha\beta}| \ll 1$, called the metric perturbation, describing the departure of the spacetime from flatness. Under the assumption of weak gravitational fields, general relativistic equations for the metric perturbation can be linearized to obtain a set of wave equations for the metric perturbation: $\Box\bar{h}_{\alpha\beta} = 16\pi T_{\alpha\beta}$, where $2\bar{h}_{\alpha\beta} \equiv 2h_{\alpha\beta} - \eta_{\alpha\beta}h^{\mu}_{\mu}$ and $\Box$ is the wave operator, $\Box \equiv \eta^{\alpha\beta}\partial_\alpha\partial_\beta$, and $T_{\alpha\beta}$ is the energy-momentum tensor. These equations have the formal solution

$$\bar{h}_{\alpha\beta}(t, \mathbf{x}) = 4\int \frac{T_{\alpha\beta}(t - |\mathbf{x} - \mathbf{x}'|, \mathbf{x}')\mathrm{d}^3x'}{|\mathbf{x} - \mathbf{x}'|}. \qquad (1)$$

Now the metric perturbation at the field point $\mathbf{x}$ at time t is determined by the configuration of the source $T_{\alpha\beta}$ at a retarded time $t - |\mathbf{x} - \mathbf{x}'|$ (recall that we are using units in which the speed of light is unity). Hence disturbances in the source travel only at a finite speed. Indeed, any non-stationary source $T_{\alpha\beta}$ will give rise to wave-like solutions for the potentials $\bar{h}_{\alpha\beta}$, which extract energy, momentum and angular-momentum from the source, propagating at the speed of light.

Effect of gravitational waves on matter

Just as in EM theory, there are only two independent polarizations of the field, denoted as h_+ (h-plus) and $h_\times$ (h-cross), and not 10 components as one might expect from the tensorial nature of $h_{\alpha\beta}$. This is because the theory is generally covariant and there are gauge degrees of freedom.

A wave of plus-polarization travelling along, say, z-axis continuously deforms a circular ring of beads in the x–y plane, taking the ring from a circle to an ellipse with its semi-major axis first oriented along, say, the x-axis after one-quarter of the wave, then along the y-axis after three-quarter and so on. Monitoring the distance from the centre of the ring to the beads at the ends of two orthogonal radial directions can best measure the deformation of the ring. This is the principle behind a laser interferometer antenna. If the ring's original radius was R the semi-major and semi-minor axes of the ellipse would be $(1 + h/2)R$ and $(1 - h/2)R$, respectively. A wave of cross-polarization has similar effect but the whole pattern of deformation gets rotated by $\pi/4$: This contrasts with the oscillatory response of a single charged particle to an EM wave and the two polarizations of light are at an angle of $\pi/2$ relative to each other.

Gravitational wave interferometers are quadrupole detectors with a good sky coverage. A single antenna, except when it is a spherical resonant detector, cannot determine the polarization state of a transient wave or the direction to the source that emits the radiation. Interferometers or resonant bars don't measure the two polarizations separately but rather a linear combination of the two given by:

$$h(t) = F_+(\theta, \varphi, \psi)h_+(t) + F_\times(\theta, \varphi, \psi)h_\times(t), \qquad (2)$$

where F_+ and $F_\times$ are the antenna patterns. To infer the direction (θ, φ) to the source, the polarization amplitudes $(h_+, h_\times)$, and the polarization angle ψ, it is necessary to make five measurements, which is possible with three interferometers: each interferometer gives a response, say $h_1(t)$, $h_2(t)$, and $h_3(t)$, and one can infer two independent delays, say $t_1 - t_2$, and $t_2 - t_3$, in the arrival times of the transient at the antennas. Therefore, a network of antennas, geographically widely separated so as to maximize the time delays and hence improve directionality, is needed for GW observations. Moreover, detecting the same event in two or more instruments helps to remove the non-Gaussian and non-stationary backgrounds, while adding a greater degree of confidence to the detection of an event. In the case of continuous waves and stochastic backgrounds the motion of the detector relative to the source causes a Doppler modulation of the response which can be de-convolved from the data to fully reconstruct the wave (as one would in the case of a point source) or reconstruct a map of the sky (as one would in the case of a stochastic background).

Amplitude, luminosity and frequency

The amplitude h and luminosity L of a source of GW is given in terms of the famous quadrupole formula (see for details, e.g. ref. 3):

$$h_{mn}(t, \mathbf{r}) = \frac{2}{r}\ddot{I}_{mn}(t - \mathbf{r}), \qquad \mathsf{L} = \frac{1}{5}\langle \dddot{I}_{mn}\dddot{I}^{mn}\rangle, \qquad (3)$$

where an overdot denotes derivative with respect to time; angular brackets denote a suitably defined averaging process (say, over a period of the GW); I_{mn} is the reduced (or trace-free) quadrupole moment tensor which is related to the usual quadrupole tensor $I^{mn} \equiv \int T^{00} x^m x^n \mathrm{d}^3x$; via $I_{mn} \equiv I_{mn} - \delta_{mn} I^k_k/3$. In simple terms, for a source of size R, mass M and angular frequency ω; located at a distance r from Earth,

$$h \sim \varepsilon_h \frac{M}{r} R^2 \omega^2, \quad \mathsf{L} \sim \varepsilon_L M^2 R^4 \omega^6. \tag{4}$$

where $\varepsilon_{h,\mathsf{L}}$ are dimensionless efficiency factors that depend on the orientation of the system relative to the observer (in the case of h only) and how deformed from spherical symmetry the system is. $\varepsilon_{h,\mathsf{L}} \sim 1$ for ideally oriented and highly deformed sources. The amplitude of the waves, just as in the case of electro-magnetic radiation, decreases as inverse of the distance to the source. However, there is a crucial difference between EM and GW observations that is worth pointing out: Let r_l be the largest distance from which an EM or a GW detector can observe standard candles. In the case of EM telescopes r_l is limited by the smallest flux observable, which falls off as the inverse-square of the distance. This is because astronomical EM radiation is the superposition of waves emitted by a large number of microscopic sources, each photon with its own phasing; we cannot follow each wave separately but only a superposition of many of them. This, of course, is the reason why in conventional astronomy the number counts of standard candles increase as $r_l^{3/2}$. In the case of GW, signals we expect to observe are emitted by the coherent bulk motion of large masses and hence it is possible to observe each cycle of the wave as it passes through the antenna. Indeed, one can fold many wave cycles together to enhance the visibility of the signal buried in noise, provided the shape of the signal is known beforehand. Because we can follow the amplitude of a wave the number of sources which an antenna can detect increases as r_l^3.

For a self-gravitating system, say a binary system of two stars of masses m_1 and m_2 (total mass $M = m_1 + m_2$ and symmetric mass ratio $\eta = m_1 m_2/M^2$), the linear velocity v and angular velocity ω are related to the size R of the system via Keplar's laws: $\omega^2 = M/R^3$; $v^2 = M/R$. It turns out that the efficiency factors for such a system are $\varepsilon_h = 4\eta C$; $\varepsilon_L = 32\eta^2/5$, so that

$$h \simeq 4\eta C \frac{M}{r}\frac{M}{R}, \quad \mathsf{L} \simeq \frac{32}{5}\eta^2 v^{10}, \quad f_{\mathrm{GW}} = 2 f_{\mathrm{orb}}, \tag{5}$$

where $C \sim 1$ is a constant that depends on the orientation of the source relative to the detector, f_{GW} is the GW frequency which is equal to twice the orbital frequency f_{orb}. The above relations imply that the amplitude of a source is greater the more compact it is and the luminosity is higher from a source that is more relativistic. The factor to covert the luminosity from $G = c = 1$ units to conventional units is $\mathsf{L}_0 \equiv c^5/G \simeq 3.6 \times 10^{59}$ erg s^{-1}. Since $v < 1$, L_0 denotes the best luminosity a source could ever have and generally $\mathsf{L} \ll \mathsf{L}_0$.

3. Gravitational wave detector projects

There are chiefly two types of GW detectors that are currently in operation taking sensitive data: (i) resonant bars and (ii) laser interferometers. The sensitivity of a detector is defined in terms of the smallest discernible dimensionless strain caused by an astronomical source against background noise of the instrument. Because a GW antenna can follow the phase of GW, the sensitivity of an antenna is given in terms of the amplitude noise spectral density as a function of frequency and is measured in Hz$^{-1/2}$. Figure 1 shows in solid lines the design sensitivity goals of three generations of ground-based interferometers (shown here for the American initial and advanced LIGO, and European Advanced VIRGO). The left panel shows the same for the space-based LISA. Also plotted in Figure 1 are source strengths to be discussed in §4.

Ground-based interferometers

Ground-based interferometers are sensitive in the frequency band of 10–1000 Hz (see ref. 4 for a fuller description). In a laser interferometric antenna the tidal deformation caused in the two arms of a Michelson interferometer is sensed as a shift in the fringe pattern at the output port of the interferometer. The sensitivity of such a detector is limited at low frequencies (10–40 Hz) by anthropogenic sources and seismic disturbances, at intermediate frequencies (40–300 Hz) by thermal noise of optical and suspended components, and at high frequencies (>300 Hz) by photon shot noise. Three key technologies have made it possible to achieve the current level of sensitivities: (1) An optical layout that makes it possible to recycle the laser light exiting the interferometer and build effective powers that are 100–1000's of times larger than the input thereby mitigating the photon shot noise. This technique allows to operate the interferometer either in the wide band mode (as in Figure 1), or with a higher sensitivity in a narrow band of about 10–50 Hz centered at a desired frequency, say 500 Hz, but at the cost of worsened sensitivity over the rest of the band. This latter mode of operation is called signal recycling and is particularly useful for observing long-lived continuous wave sources. (2) Multiple suspension systems that filter the ground motion and keep the mirrors essentially free from seismic disturbances. (3) Monolithic suspensions that help isolate the suspension thermal noise to a narrow frequency band.

There are currently six long baseline detectors in operation: The American Laser Interferometer Gravitational-Wave

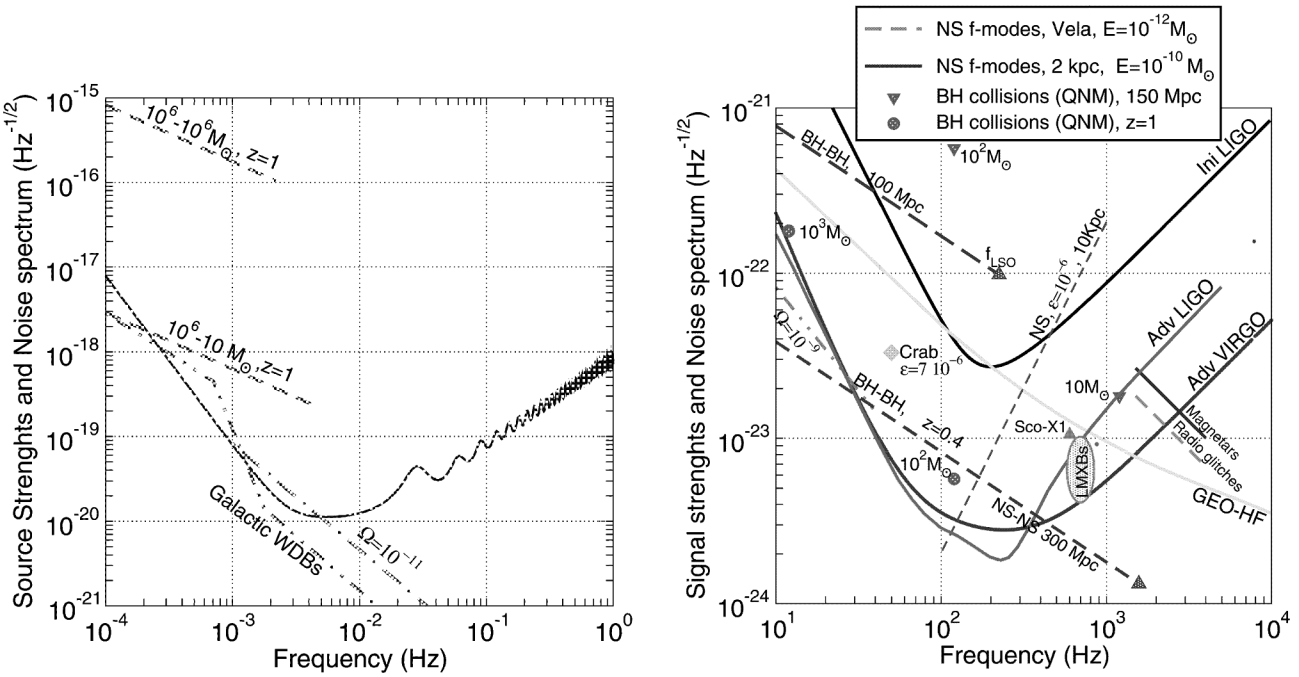

Figure 1. Amplitude noise spectrum (in $Hz^{-1/2}$) of space-based LISA (left panel) and two generations of ground-based interferometers, initial LIGO and advanced LIGO, advanced VIRGO and GEO-HF. Also plotted on the same graph are the source strengths for archetypal binary, continuous and stochastic radiation in the same units. A source will be visible in a network of 3 interferometers if it is roughly 5 times above the noise PSD.

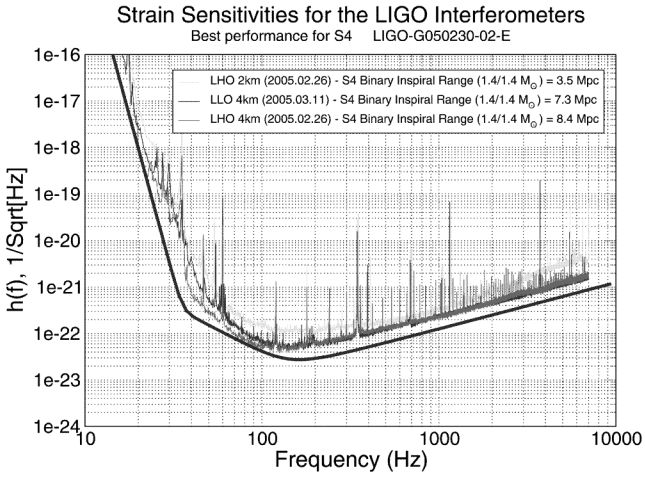

Figure 2. Amplitude noise spectrum (in $Hz^{-1/2}$) of LIGO interferometers during the fourth science run S4. At this time the LIGO instruments were roughly within a factor of 2 of their design goal.

Observatory (LIGO)[5], which is a network of three detectors, two with 4 km arms and one with 2 km arms, at two sites (Hanford, Washington and Livingstone, Louisiana), the French-Italian VIRGO detector with 3 km arms at Pisa[6], the British-German GEO600 (ref. 7) with 600 m arms at Hannover and the Japanese TAMA with 100 m arms in Tokyo[8]. Australia has built a 80 m test facility with a plan to build a km-size detector sometime in the future. The American LIGO detectors are already close to their design sensitivity. Figure 2 shows the sensitivity of these detectors during the fourth science run (called S4). The GEO600 and Virgo detectors are expected to operate at their design sensitivity during the course of the next year. LIGO detectors have begun a year long science run, to be joined in due course by GEO600, TAMA and Virgo. The data from the worldwide network will be the best ever, providing a real chance for a first direct detection.

Plans are well already underway both in Europe and the USA to build, by 2010–2013, the next generation of interferometers that are 10–15 times more sensitive than the initial interferometers or to enhance the sensitivity in the kHz region where we can expect to observe neutron star cores and quasi-normal modes of stellar mass black holes. With a peak sensitivity of $h \sim 10^{-24}\ \mathrm{Hz}^{-1/2}$ the advanced LIGO and VIRGO detectors will be able to detect NS ellipticities in the range 10^{-6}–10^{-8} from sources in our Galaxy, BH-BH binaries of total mass 50 $M_\odot$ at a redshift of $z \sim 0.5$; and stochastic background at the level of $\Omega_{GW} \sim 10^{-9}$. The high-frequency upgrade of GEO600, called GEO-HF, is designed to look at normal mode oscillations of neutron stars, believed to result from star quakes and believed to be the root cause of glitches in pulsar timing when the frequency of the pulsar seems to suddenly increase.

In the longer term, over the next 10 to 15 years, we might see the development of 3rd generation GW antennas. The sensitivity of the current and next generation instruments is still far from the fundamental limitations of a ground-based detector: The gravity gradient noise at low frequencies

due to natural (winds, clouds, earthquakes) and anthropogenic causes, and the quantum uncertainty principle of mirror position at high frequencies. A detector subject to only these limitations requires the development of new optical and cryogenic techniques that form the foundation of a third generation GW detector that is currently undergoing a design study.

Space-based interferometers

Laser Interferometer Space Antenna (LISA) is a joint ESA-NASA project to develop a space-based gravitational wave detector. The plan is to put in space three spacecraft in heliocentric orbit, 60 degrees behind the Earth, in an equilateral triangular formation of size 5 million km[10], scheduled to be ready by 2014. LISA's sensitivity is limited by difficulties with long time-scale ($> 10^5$ s) stability, photon shot-noise at high frequencies ($\sim 10^{-3}$ Hz) and large size ($> 10^{-1}$ Hz). LISA will be able to observe Galactic, extra-Galactic and cosmological point sources as well as stochastic backgrounds from different astrophysical populations and perhaps from certain primordial processes. Feasibility studies are now underway to assess the science case and technology readiness for covering the frequency gap of LISA and ground-based detectors. The Deci-Hertz Interferometer Gravitational-Wave Observatory (DECIGO)[11] by the Japanese team and the Big-Bang Observer (BBO), a possible follow-up of LISA[12], are aimed as instruments to observe the primordial GW background and to answer cosmological questions on the expansion rate of the Universe and dark energy.

4. Sources of gravitational waves

Gravitational wave detectors will unveil dark secrets of the Universe by helping us to study sources in extreme physical environs: strong non-linear gravity, relativistic motion, extremely high density, temperature and magnetic fields, to list a few. We shall focus our attention on compact objects (in isolation or in binaries) and stochastic backgrounds.

Compact binaries

An astronomical binary, in which the stars orbit about their common center-of-mass, emits gravitational radiation. The loss in energy in the form of gravitational waves leads to an inspiral of the orbits leading eventually to the coalescence of the two stars. This will be associated with a burst of gravitational waves. Massive black holes believed to exist at galactic cores could merge with similar black holes at the cores of other galaxies when galaxies collide leading to a burst of gravitational radiation. Binary coalescences are believed to be a major source of gravitational radiation.

Compact binaries, consisting of a pair of compact objects (i.e. NS and/or BH), are an astronomer's standard candles[13]: A parameter called the chirp mass $\mathcal{M} \equiv \eta^{2/3} M$, completely fixes the absolute luminosity of the system. Hence, by observing GW from a binary we can measure the luminosity distance to the source provided the source chirps, that is the orbital frequency changes, by as much as $1/T$ during an observational period T. This feature helps to accurately measure cosmological parameters and their variation as a function of red-shift. The dynamics of a compact binary consists of three phases: (i) inspiral, (ii) plunge and (iii) merger. In the following we will discuss each in turn.

The early inspiral phase. This is the phase in which the a binary spends 100's of millions of years and the power emitted in GW is low. This phase can be treated using linearized Einstein's equations and post-Newtonian theory with the energy radiated into gravitational waves balanced by a loss in the binding energy of the system. The emitted GW signal has a characteristic shape with its amplitude and frequency slowly increasing with time and is called a chirp waveform. Formally, the inspiral phase ends at the last stable orbit (LSO) when the effective potential of the system undergoes a transition from having a well-defined minimum to the one without a minimum, after which stable orbits can no longer be supported. This happens roughly when the two objects are separated by $R \simeq 6GM/c^2$; or when the frequency of GW is $f_{\rm LSO} \simeq 4400\ (M_\odot/M)$ Hz. The signal power drops as $f^{-7/3}$ and the photon shot-noise in an interferometer increases as f^2 beyond about 200 Hz so that it will only be possible to detect a signal in the range from about 10 to 500 Hz (and a narrower bandwidth of 40–300 Hz in initial interferometers) during which the source brightens up half-a-million fold (recall that the luminosity $\propto v^{10} \propto f^{10/3}$). For $M \lesssim 10\, M_\odot$, inspiral phase is the only phase sensed by the interferometers and lasts for a duration of $\tau = 5576\, \eta^{-1}\ (M/M_\odot)^{-5/3}$ s, starting at 10 Hz. The phase development of the signal is very well modelled during this epoch and one can employ matched filtering technique to enhance the visibility of the signal by roughly the square root of the number of signal cycles $N_{\rm cyc} \sim 16\tau$; starting at 10 Hz. Since a large number of cycles are available it is possible to discriminate different signals and accurately measure the parameters of the source such as its location (a few degrees each in co-latitude and azimuth)[14], mass (fractional accuracy of 0.05–0.3% in total mass and a factor 10 worse for reduced mass, with greater accuracy for NS than BH), and spin (to within a few percents)[15].

The late inspiral, plunge and merger phase. This is the phase when the two stars are orbiting each other at a third of the speed of light and experiencing strong gravitational fields with the gravitational potential being $\varphi = GM/Rc^2 \sim 0.1$. This phase warrants the full non-linear structure of Ein-

stein's equations as the problem involves strong relativistic gravity, tidal deformation (in the case of BH-BH or BH-NS) and disruption (in the case of BH-NS and NS-NS) and has been the focus of numerical relativists[16] for more than two decades. However, some insights have been gained by the application of advanced mathematical techniques aimed at accelerating the convergence properties of post-Newtonian expansions of the energy and flux required in constructing the phasing of GW[17–19]. This is also the most interesting phase from the point of view of testing non-linear gravity as we do not yet fully understand the nature of the two-body problem in general relativity. Indeed, even the total amount of energy radiated during this phase is highly uncertain, with estimates in the range 10% (ref. 20) to 0.07% (ref. 18). Since the phase is not well-modelled, it is necessary to employ sub-optimal techniques, such as time-frequency analysis, to detect this phase and then use numerical simulations to gain further insights into the nature of the signal.

The late merger phase. This is the phase when the two systems have merged to form either a single NS or a BH, settling down to a quiescent state by radiating the deformations inherited during the merger. The emitted radiation can be computed using perturbation theory and gives the quasi-normal modes (QNM) of BH and NS. The QNM carry a unique signature that depends only on the mass and spin angular momentum in the case of BH, but depends also on the equation-of-state (EOS) of the material in the case of NS. Consequently, it is possible to test conclusively whether or not the newly born object is a BH or NS: From the inspiral phase it is possible to estimate the mass and spin of the object quite precisely and use that to infer the spectrum of normal modes of the BH. The fundamental QNM of GW from a spinning BH, computed numerically and then fitted, is[21] $f_{\rm QNM} = 750[1 - 0.63\ (1 - a)^{0.3}]$ $(100M_\odot/M)$ Hz, with a decay time of $\tau = 5.3/[f_{\rm QNM}(1 - a)^{0.45}]$ ms, where a is the dimensionless spin parameter of the hole taking values in the range [0, 1]. The signal will be of the form $h(t; \tau, \omega) = h_0 e^{-t/\tau} \cos(\omega t)$; $t \geq 0$; h_0 being the amplitude of the signal that depends on how deformed the hole is.

It has been argued that during the late stages of merger the energy emitted in the form of QNM might be as large as 3% of the system's total mass[20]. By matched filtering, it should be possible to detect QNM resulting from binary mergers of mass in the range $60–10^3\ M_\odot$ at a distance of 200 Mpc in initial LIGO and from $z \sim 2$ in advanced LIGO. In Figure 1 filled circles show the amplitude and frequency of QNM radiation from a source at $z = 1$; and total mass 1000 or $100\ M_\odot$. Such signals should serve as a probe to test if massive black holes found at galactic cores initially formed as small BHs of $10^3\ M_\odot$ and then grow by rapid accretion. Moreover, there is a growing evidence[22] that globular clusters might host BH of mass $M \sim 10^3\ M_\odot$ at their cores. If this is indeed true then the QNM from activities associated with such BHs would be observable in the local Universe, depending on how much energy is released into GW when other objects fall in.

The span of an interferometer to binaries varies with the masses as $\eta^{1/2}M^{5/6}$, greater asymmetry in the masses reduces the span but larger total mass increases the span. In Figure 3 we have plotted the distance up to which binaries can be seen as a function of the binary's total mass for an equal mass system when including both the inspiral and merger part of the signal. This estimate is based on the effective-one-body approach[18,23] which predicts 0.07% of the total mass in the merger waves.

1. NS-NS binaries. Double NS coalescences can be seen in initial LIGO to a distance of about 15 Mpc and in advanced LIGO to a distance of 300 Mpc as shown in Figure 1. Based on the observed small population of binary NS that merge within the Hubble time, Kalogera *et al.*[2,24] conclude that the Galactic coalescence rate is $\sim 1.8 \times 10^{-4}\ \mathrm{yr}^{-1}$, which would imply an event rate of NS-NS coalescences is 0.25 and $1500\ \mathrm{yr}^{-1}$, in initial and advanced LIGO, respectively. As the spins of NS are very small ($a \ll 1$) and because the two stars would merge well outside the LIGO's sensitivity band, the current state-of-the-art theoretical waveforms[25] will serve as good templates for matched filtering. However, detailed relativistic hydrodynamical simulations (see, e.g. ref. 26) would be needed to interpret the emitted radiation during the coalescence phase, wherein the two stars collide to form a bar-like structure prior to merger. The bar hangs up over a couple of dynamical time-scales to get rid of its deformity by emitting strong bursts of GW. Observing the radiation from this phase should help to deduce the EOS of NS bulk matter. Also, an event rate as large as in advanced LIGO and EURO will be a valuable catalogue to test astronomical predictions, for example if γ-ray bursts are associated with NS-NS or NS-BH mergers[27].

2. NS-BH binaries. These are binaries consisting of one NS and one BH and are very interesting from an astrophysical point of view. The initial evolution of such systems can be treated analytically fairly well, however, the presence of a BH with large spin can cause the NS to be whirled around in precessing orbits due to the strong spin-orbit coupling. The evolution of such systems is really not very well understood. However, it should be possible to use the 'point-mass' approximation in which the NS is treated as a point-particle orbiting a BH, in getting some insight into the dynamics of the system. The evolution will also be complicated by the tidal disruption of the NS before reaching the last stable orbit. It should be possible to accurately measure the onset of the merger phase and deduce the radius of the NS to ~ 15% and thereby infer the EOS of NS[28].

Advanced interferometers will be sensitive to NS-BH binaries out to a distance of about 650 Mpc. The rate of coalescence of such systems is not known empirically as

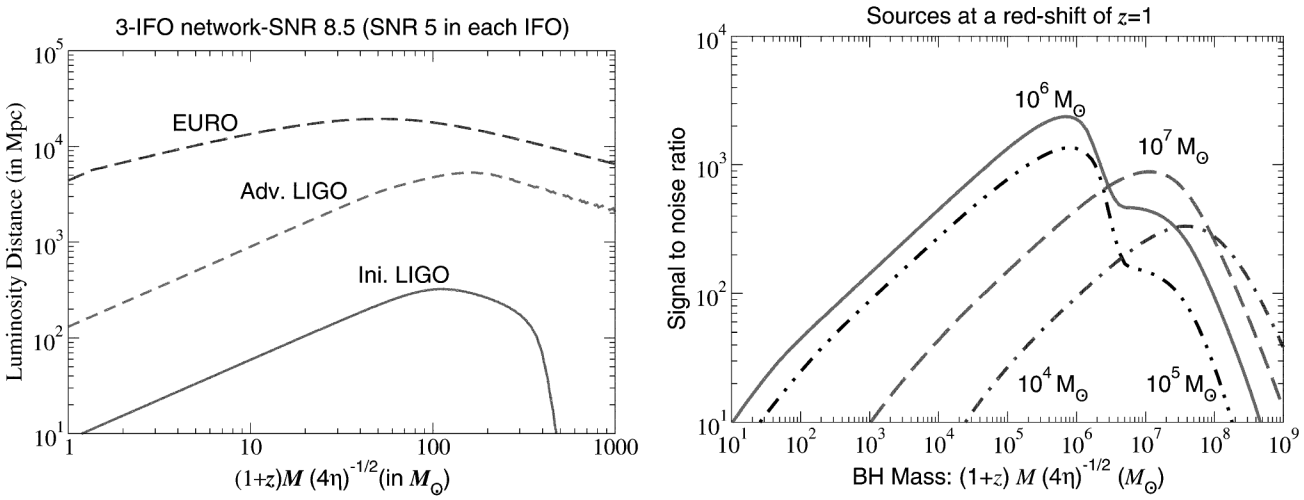

Figure 3. The first plot shows the span of initial and advanced LIGO and EURO for compact binary sources when including both the inspiral and merger waveforms in our search algorithms. BH mergers can be seen out to a red-shift of $z = 0.55$ in advanced LIGO and $z = 2$ in EURO. In the second plot we show the SNR achieved by LISA for inspiral signals from supermassive black hole binaries at $z = 1$. The plot shows the SNR for different masses of the primary black hole as a function of the secondary black hole's mass.

there have been no astronomical NS-BH binary identifications. However, the population synthesis models give[29] a Galactic coalescence rate in the range 3×10^{-7}–5×10^{-6} yr^{-1}. The event rate of NS-BH binaries will be worse than BH-BH of the same total mass by a factor of $(4\eta)^{3/2}$ since the SNR goes down as $\sqrt{4\eta}$. Taking these factors into account we get an optimistic detection rate of NS-BH of 0.05 and 400 per year in initial and advanced LIGO, respectively.

3. BH-BH binaries. Black hole mergers are the most promising candidate sources for a first direct detection of GW. These sources are the most interesting from the viewpoint of general relativity as they constitute a pair of interacting Kerr spacetimes experiencing the strongest possible gravitational fields before they merge with each other to form a single BH, and serve as a platform to test general relativity in the non-linear regime. For instance, one can detect the scattering of GW by the curved geometry of the binary[30,31], and measure, or place upper limits on, the mass of the graviton to 2.5×10^{-22} eV and 2.5×10^{-26} eV in ground- and space-based detectors, respectively[32]. High SNR events (which could occur once every month in advanced LIGO) can be used to test the full non-linear gravity by comparing numerical simulations with observations and thereby gain a better understanding of the two-body problem in general relativity. As BH binaries can be seen to cosmological distances, a catalogue of such events compiled by LIGO can be used to measure cosmological parameters (Hubble constant, expansion of the Universe, dark energy) and test models of cosmology[27].

The span of interferometers to BH-BH binaries varies from 100 Mpc (with the inspiral signal only) to 150 Mpc (inspiral plus merger signal) in initial LIGO and to a red-shift of $z = 0.4$–0.55 in advanced LIGO, and $z = 2$ in EURO (cf. Figures 1 and 3). As in the case of NS-BH binaries, here too there is no empirical estimate of the event rate. Population synthesis models are highly uncertain about the Galactic rate of BH-BH coalescences and predict[29] a range of 3×10^{-8}–10^{-5} yr^{-1}; which is smaller than the predicted rate of NS-NS coalescences. However, owing to their greater masses, BH-BH event rate in our detectors is larger than NS-NS by a factor $M^{5/2}$ for $M \lesssim 100\, M_\odot$. The predicted event rate is a maximum of 1 yr^{-1} in initial LIGO and 500 yr^{-1} to 20 day^{-1} in advanced LIGO.

4. Massive black hole binaries. It is now believed that the centre of every galaxy hosts a BH whose mass is in the range 10^6–$10^9\, M_\odot$ (ref. 33). These are termed as massive black holes (MBH). There is now observational evidence that when galaxies collide the MBH at their nuclei might get close enough to be driven by gravitational radiation reaction and merge within the Hubble time[34]. For a binary with $M = 10^6\, M_\odot$ the frequency of GW at the last stable orbit is $f_{\rm LSO} = 4$ mHz, followed by merger from 4 mHz to the QNM at 24 mHz (if the spin of the black holes is negligible). This is in the frequency range of LISA which has been designed to observe the MBH: their formation, merger and activity.

The SNR for MBH-MBH mergers in LISA is shown in Figure 3. These mergers will appear as the most spectacular events requiring no templates for signal identification, although good models would be needed to extract source parameters. Supermassive black hole mergers can be seen almost whereever they occur; one can observe galaxy mergers throughout the Universe and address astrophysical questions about the origin, growth and population of MBH. The recent discovery of a MBH binary[34] and the association of X-shaped radio lobes with the merger of MBH[35] has raised the optimism concerning MBH mergers and the predicted rate for MBH mergers is the same as the rate at

which galaxies merge, about 1 yr^{-1} out to a red-shift of $z = 5$ (ref. 36).

5. Smirches. The MBH environment of our own galaxy is known to constitute a large number of compact objects and white dwarfs. Three-body interaction will occasionally drive these compact objects, white dwarfs and other stars into a capture orbit of the central MBH. The compact object will be captured in an highly eccentric trajectory ($e > 0.99$) with the periastron close to the last stable orbit of the MBH. Due to relativistic frame dragging, for each passage of the apastron the compact object will experience several turns around the MBH in a near circular orbit. Therefore, long periods of low-frequency, small-amplitude radiation will be followed by several cycles of high-frequency, large-amplitude radiation. The apastron slowly shrinks, while the periastron remains more or less at the same location, until the final plunge of the compact object before merger. There is a lot of structure in the waveforms which arises as a result of a number of different physical effects: Contribution from higher order multipoles, precession of the orbital plane that changes the polarization of the waves observed by LISA, etc. This complicated structure smears the power in the signal in the time-frequency plane[37] as compared to a sharp chirp from a non-spinning BH binary and for this reason this spin modulated chirp is called a smirch[38].

As the compact object tumbles down the MBH it will sample the spacetime geometry in which it is moving and the structure of that geometry will imprint in the GW emitted in the process. By observing smirches, LISA offers a unique opportunity to directly map the spacetime geometry around the central object and test whether or not this structure is in accordance with the expectations of general relativity[39]. Indeed, according to Einstein's theory the geometry of a rotating black hole is uniquely determined to be the Kerr metric involving just two parameters, the mass of the MBH and its spin. Thus, the various multipole-moments of the source are uniquely fixed once we have measured the mass and spin of the BH. With the observed smirch one can basically test (i) whether general relativity correctly describes the spacetime region around a generic BH and (ii) if the central object is indeed a BH or some other exotic matter.

The SNR from smirches will be between 10 and 50 depending on the mass of the central object (cf. Figure 3) but it might be very difficult to match filter them due to their complicated shapes. The event rate is expected to be rather high. Indeed, a background population of these smirches will cause confusion noise and only sources in the foreground will be visible in LISA. The foreground event rate is somewhat uncertain, ranging from 1–10 yr^{-1} within 1 Gpc (ref. 40).

Neutron stars. Neutron stars are the most compact stars in the Universe. With a density of 2×10^{14} g cm^{-3}, and surface gravity $\varphi \equiv M/R \sim 0.1$, they are among the most exotic objects whose composition, equation-of-state and structure, are still largely unknown. Being highly compact they are potential sources of GW. The waves could be generated either from the various normal modes of the star, or because the star has a tiny deformation from spherical symmetry and is rotating about a non-axisymmetric axis, or because there are density inhomogeneities caused by an environment, or else due to certain relativistic instabilities. We will consider these in turn.

1. Supernovae and birth of NS. The birth of a NS is preceded by the gravitational collapse of a highly evolved star or the core collapse of an accreting white dwarf. Type II supernovae (SN) are believed to result in a compact remnant. In any case, if the collapse is non-spherical then GW could carry away some of the binding energy and angular momentum depending on the geometry of the collapse. It is estimated that in a typical SN, GW might extract about 10^{-7} of the total energy[41]. The waves could come off in a burst whose frequency might lie in the range ~ 200–1000 Hz. Advanced LIGO will be able to see such events up to the Virgo supercluster with an event rate of about 30 per year.

2. Equation of state and normal modes of NS. In order to determine the equation of state (EOS) of a neutron star, and hence its internal structure, it is necessary to independently determine its mass and radius. Astronomical observations cannot measure the radius of a neutron star although radio and X-ray observations do place a bound on its mass. Therefore, it has not been possible to infer the EOS. Neutron stars will have their own distinct normal modes and GW observations of these modes should resolve the matter here since by measuring the frequency and damping times of the modes it would be possible to infer both the radius and mass of NS. The technique is not unlike helioseismology where observation of normal modes of the Sun has facilitated insights into its internal structure. In other words, GW observations of the normal modes of the NS will allow *gravitational asteroseismology*[42].

Irrespective of the nature of the collapse a number of normal modes will be excited in a newly formed NS. The star will dissipate the energy in these modes in the form of GWs as a superposition of the various normal modes and soon the star settles down to a quiescence state. Normal modes could also be excited in old NS because of the release of energy from star quakes. The strongest of these modes, the ones that are important for GW observations, are the *p*-and *w*-modes for which the restoring forces are the fluid pressure and space-time curvature, respectively. Both of these modes will emit transient radiation which has a generic form of a damped sinusoid: $h(t; \nu, \tau) = h_0 \exp(-t/\tau)\sin(2\pi\nu t)$, where h_0 is the amplitude of the wave that depends on the external perturbation that excites the mode and ν and τ are the frequency and damping

time of the mode, respectively, and are determined by the mass and radius of the NS for a given EOS.

To make an order-of-magnitude estimate let us assume that the mass of the NS is $M_* = 1.4\ M_\odot$ and that its radius is $R_* = 10$ km. For the p-modes, which are basically fluid modes, the frequency of the fundamental mode, also called the f-mode, is simply the dynamical frequency of the fluid, namely $\nu_f \sim \sqrt{\rho}$, where ρ is the density of the fluid. For a NS of radius R_* and mass M_* this corresponds to a frequency of $\sqrt{3M_*/(4\pi R_*^3)} \sim 3$ kHz: If the star radiates all the energy deposited in the mode at a luminosity L, the damping time of the mode would be $\tau \sim E/L$: Since $E \propto M_*^2/R_*$ and $L \propto M_*^2 R_*^4 \omega^6 = M_*^5/R_*^5$, we get $\tau \sim R_*^4/M_*^3$. Indeed, detailed mode calculations for various EOS have been fitted to yield the following relations for f-modes[42]

$$\nu_f = \left[0.78 + 1.635\left(\frac{M_*}{R_*^3}\right)^{1/2}\right] \text{kHz},$$

$$\tau_f^{-1} = \frac{M_*^3}{R_*^4}\left[22.85 - 14.65\frac{M_*}{R_*}\right] \text{ s}, \qquad (6)$$

and similarly for w-modes. The f- and w-mode frequencies nicely separate into two distinct groups even when considering more than a dozen different EOS: The f-modes are in the frequency range 1–4 kHz, w-modes are in the range 8–14 kHz, and therefore, detecting a signal at these frequencies places it in one or the other category. The frequency and damping time, together with the relations above, can then be used to fix the radius and mass of the star. Observing several systems should then yield a mass-radius curve which is distinct for each EOS and thereby helps to address the question of NS structure.

In a typical gravitational collapse the amount of energy expected to be deposited in f- or w-modes, $\sim 10^{-8}\ M_\odot$, makes it impossible to detect them in initial LIGO and barely in advanced LIGO instruments, even for a Galactic source (lines marked 'magnetar' and 'radio glitches'). However, Advanced Virgo and GEO-HF should be able to detect these systems with a high SNR.

3. Relativistic instabilities in NS. NS suffer dynamical and secular instabilities caused by hydrodynamical and dissipative forces, respectively. What is of interest to us is the secular instability driven by gravitational radiation. GW emission from a normal mode in a non-spinning NS would always lead to the decay of the mode. However, the situation might reverse under certain conditions: Imagine a NS spinning so fast that a normal mode whose angular momentum (AM) in the star's rest frame is opposite to its spin, appears to an inertial observer to be co-rotating with the spin. In the inertial frame, GW extracts positive AM from the mode; therefore the mode's own AM should become more negative. In other words, the amplitude of the mode should grow as a result of GW emission, and hence the instability. The energy for the growth of the mode comes from the rotational energy of the star, which acts like a pump field. Consequently, the star would spin down, the mode's angular momentum with respect to the inertial observer will vanish and thereby halt the instability. It was expected that this instability, called the CFS instability[43,44], might drive the f-modes in a NS unstable, but the star should spin at more than 2 kHz (the smallest f-mode frequency) for this to happen. Moreover, it has been shown that due to viscous damping in the NS fluid the instability would not grow sufficiently large, or sustain for long, to be observable (see e.g. ref. 42).

It was recently realized[45] that modes originating in current-multipoles, as opposed to mass-multipoles which lead to the f-mode, could be unstable even in a non-spinning NS. These modes, called the r-modes, have received a lot of interest because they could potentially explain why spin frequencies of NS in low-mass X-ray binaries are all clustered in a narrow range of 300–600 Hz or why no NS with spin periods smaller than 1.24 ms have been found. The role of r-modes in these circumstances is as yet inconclusive because the problem involves very complicated astrophysical processes (magnetic fields, differential rotation, superuidity and superconductivity), microphysics (the precise composition of NS – hyperons, quarks) and full non-linear physics of general relativity. It is strongly expected that r-modes will be emitted by newly formed NS during the first few months of their birth[42,46]. The frequency of these modes will be 4/3 of the spin frequency of the star and might be particularly important if the central object in a low-mass X-ray binary is a strange star[47]. The radiation might last for about 300 years and the signal would be detectable in initial LIGO with a few weeks of integration.

4. NS environment. A NS with an accretion disc would be spun up due to transfer of AM from the disc. Further, accretion could lead to density inhomogeneities on the NS that could lead to the emission of GW. The resulting radiation reaction torque could balance the accretion torque and halt the NS from spinning up. It has been argued[48] that GW emission could be the cause for spin frequencies of NS in low-mass X-ray binaries to be locked up in a narrow frequency range of 300–600 Hz. It is also possible that r-modes are responsible for the locking up of frequencies instead, in which case the waves would come off at a different frequency[47]. These predictions can be tested with advanced LIGO or Advanced Virgo as Sco-X1, a nearby low-mass X-ray binary, would produce quite a high SNR (marked as filled Δ in Figure 1) but also a host of other low-mass X-ray binaries (shaded ellipse) might also be observed with advanced instruments.

5. Spinning NS with asymmetries. Our galaxy is expected to have a population of 10^8 NS and they normally spin at high rates (several to 500 Hz). Such a large spin

must induce some equatorial bulge and flattening of the poles. The presence of a magnetic field may cause the star to spin about an axis that is different from the symmetry axis leading to a time-varying quadrupole moment[49]. Gravitational waves emitted by a typical NS a distance of $r = 10$ kpc from the Earth will have an amplitude[50] $h \sim 8 \times 10^{-26} f_{\mathrm{kHz}}^2 \varepsilon_{-6}$, where f_{kHz} is the frequency of GW in kHz and ε_{-6} is the ellipticity of the star in units of 10^{-6}. Figure 1 plots the signal strength expected from a NS with $\varepsilon = 10^{-6}$ at 10 kpc integrated over four months. The ellipticity of neutron stars is not known but one can obtain an upper limit on it by attributing the observed spin-down rate of pulsars as entirely due to gravitational radiation back reaction, namely that the change in the rotational energy is equal to GW luminosity. The ellipticity of the Crab pulsar inferred in this way is $\varepsilon \leq 7 \times 10^{-4}$. The GW amplitude corresponding to this ellipticity is $h \leq 10^{-24}$. Noting that Crab has a spin frequency of 25 Hz (GW frequency of 50 Hz), on integrating the signal for 10^7 s one obtains $h = 3.3 \times 10^{-21}$ Hz$^{-1/2}$, which is easily reachable by LIGO. It is unlikely that the ellipticity is so large and hence the GW amplitude is probably much less. However, seeing Crab at a hundredth of this ellipticity is quite good with advanced LIGO as indicated by a diamond in Figure 1 (Note that Crab is at 2 kpc, so with an ellipticity of $\varepsilon = 7 \times 10^{-6}$ the signal strength would be 35 times higher than the NS line.)

Stochastic background

Incoherent superposition of radiation from a population of background sources and/or quantum processes in the early Universe[29] might produce stochastic signals that would fill the whole space. By detecting such a stochastic signal we can gain knowledge about the underlying populations and physical processes. A network of antennas can be used to discover stochastic signals buried under the instrumental noise backgrounds. It is expected that the instrumental backgrounds will not be common between two geographically well-separated antennas. Thus, by cross-correlating the data from two detectors we can eliminate the background and filter the interesting stochastic signal. However, when detectors are not co-located the SNR builds only over wavelengths longer than twice the distance between antennas, which in the case of the two LIGO antennas means over frequencies $\lesssim 40$ Hz (ref. 51). The visibility of a stochastic signal integrated over a period T and bandwidth f only increases as $(fT)^{1/4}$ since cross-correlation uses a 'noisy' filter.

1. Astronomical backgrounds. There are thousands of white dwarf binaries in our galaxy with their period in the range from a few hours to ~ 100 seconds. Each binary will emit radiation at a single frequency, but over an observation period T each frequency bin of width $\Delta f = 1/T$ will be populated by many sources. Thus, unless the source is nearby it will not be possible to detect it amongst the confusion background created by the underlying population. However, a small fraction of this background population might be detectable as strong foreground sources. The parameters of many white dwarfs are known so well that we can precisely predict their SNRs in LISA and thereby use them to calibrate the antenna. In Figure 1 the curve labelled WDB (left panel) is the expected confusion noise from Galactic white dwarfs[29,52]. NS and BH populations do not produce a large enough background to be observable. Note that the white dwarf background imposes a limitation on the sources we can observe in the frequency region from 0.3 mHz to about 1 mHz – the region where we expect smirches to occur.

2. Primordial background. A cosmological background should have been created in the very early Universe and later amplified, as a result of parametric amplification, by its coupling to the background gravitational field[29]. Imprint on such a background are the physical conditions that existed in the early Universe, as also the nature of the physical processes that produced the background. Observing such a background is, therefore, of fundamental importance as this is the only way we can ever hope to directly witness the birth of the Universe. The cosmic microwave background, which is our firm proof of the hot early phase of the Universe, was strongly coupled to baryons for 350,000 years after the big bang and therefore the signature of the early Universe is erased from it. The GW background, on the other hand, is expected to de-couple from the rest of matter 10^{-24} s after the big bang, and would, therefore, carry uncorrupted information about the origin of the Universe.

The strength of stochastic GW background is measured in terms of the fraction Ω_{GW} of the energy density in GW as compared to the critical density needed to close the Universe and the amplitude of GW is given by ref. 50. $h = 8 \times 10^{-19} \Omega_{\mathrm{GW}}^{1/2}/f$, for $H_0 = 65$ km s^{-1} Mpc: By integrating for 10^7 s, over a bandwidth f, we can measure a background density at $\Omega_{\mathrm{GW}} \simeq 2 \times 10^{-6}$ in initial LIGO, 7×10^{-10} in advanced LIGO and 3×10^{-11} in LISA (cf. Figure 1 dot-dashed curves marked Ω_{GW}). In the standard inflationary model of the early Universe, the energy density expected in GW is $\Omega_{\mathrm{GW}} \lesssim 10^{-15}$, and this will not be detected by future ground-based detectors or LISA. However, space missions currently being studied (DECIGO/BBO) to exploit the astrophysically quiet band of 10^{-2}–1 Hz might detect the primordial GW and unveil the origin of the Universe.

5. Conclusions

Direct detection of gravitational radiation will be an extremely important step in opening a new window on the Universe. Interferometric and resonant mass detectors will play a key role in this step. Gravitational radiation they

observe should facilitate both quantitatively and qualitatively new tests of Einstein's theory including the measurement of the speed of gravitational waves, and hence (an upper limit on) the mass of the graviton, polarization states of the radiation, non-linear effects of general relativity untested in solar system or Hulse-Taylor binary pulsar observations, uniqueness of axisymmetric spacetimes, the mystery of galaxy formation, and so on.

The future holds other ways of observing cosmic gravitational waves. Radio astronomy promises to make it possible to observe both primordial gravitational waves and point sources. Polarization spectra of the cosmic background radiation will carry signature of the primordial waves. Future radio antennas (such as, the Square Kilometer Array) will monitor tens of thousands of pulsars which can be used as an array of high-precision clocks to observe the gravitational Universe.

1. Weisberg, J. M. and Taylor, J. H., The Relativistic Binary Pulsar B1913+16, in *Radio Pulsars* (eds Bailes, M., Nice, D. J. and Thorsett, S. E.), ASP. Conf. Series, 2003.
2. Kalogera, V. *et al*., The cosmic coalescence rates for double neutron star binaries, astro-ph/0312101, 2003.
3. Schutz, B. F., *A First Course in General Relativity*, Cambridge University Press, Cambridge, 1985.
4. Schutz, B. F., *Class. Quantum Grav*., 1999, **16**, A131.
5. Abramovici, A. *et al*., *Science*, 1992, **256**, 325.
6. Caron, B. *et al*., *Class. Quantum Grav*., 1997, **14**, 1461.
7. Lück, H. *et al*., *Class. Quantum Grav*., 1997, **14**, 1471.
8. Tsubono, K., in *First Edoardo Amaldi Conference on Gravitational Wave Experiments*, World Scientific, Singapore, 1995, p. 112.
9. EURO – Europe's Third Generation Gravitational Wave Observatory, http://www.astro.cf.ac.uk/geo/euro/
10. Bender, P. *et al*., LISA: Pre-Phase A Report, MPQ 208, Max-Planck-Institut für Quantenoptik, Garching, Germany, Second Edition, July 1998.
11. Takahashi, R. and Nakamura, T., *Astrophys. J.*, 2003, **596**, L231–L234.
12. Big Bang Observer, 2003, http://universe.gsfc.nasa.gov/program/bbo.html
13. Schutz, B. F., *Nature*, 1986, **323**, 310.
14. Jaranowski, P., Kokkotas, K. D., Krolak, A. and Tsegas, G., *Class. Quant. Grav*., 1996, **13**, 1279.
15. Cutler, C. and Flanagan, É. É., *Phys. Rev. D.*, 1994, **49**, 2658.
16. Bruegmann, B., *Ann. Phys.*, 2000, **9**, 227–246.
17. Buonanno, A. and Damour, T., *Phys. Rev. D.*, 1999, **59**, 084006.
18. Buonanno, A. and Damour, T., *Phys. Rev. D.*, 2000, **62**, 064015.
19. Damour, T., Iyer, B. R. and Sathyaprakash, B. S., *Phys. Rev. D.*, 1998, **57**, 885.
20. Flanagan, É. É. and Hughes, S., *Phys. Rev. D.*, 1998, **57**, 4535.
21. Echeverria, F., *Phys. Rev. D.*, 1989, **40**, 3194.
22. Gerssen, J. *et al*., *Astrophys. J.*, 2002 (in press) astro-ph/0210158.
23. Damour, T., Iyer, B. R. and Sathyaprakash, B. S., *Phys. Rev. D.*, 2001, **63**, 044023.
24. Burgay, M. *et al*., *Nature*, 2004, **426**, 531–533.
25. Blanchet, L., *Living Rev. Rel.*, 2002, **5**, 3.
26. Kawamura, M., Oohara, K. and Nakamura, T., General Relativistic Numerical Simulation on Coalescing Binary Neutron Stars and Gauge-Invariant Gravitational Wave Extraction, 2003, astro-ph/0306481.
27. Finn, L. S., *Phys. Rev. D.*, 1996, **53**, 2878.
28. Vallisneri, M., *Phys. Rev. Lett.*, 2000, **84**, 3519.
29. Grishchuk, L. P. *et al*., *Phys. Usp*., 2001, **44**, 1.
30. Blanchet, L. and Sathyaprakash, B. S., *Class. Quant. Grav*., 1994, **11**, 2807.
31. Blanchet, L. and Sathyaprakash, B. S., *Phys. Rev. Lett.*, 1995, **74**, 1067.
32. Will, C. M., *Phys. Rev. D.*, 1998, **57**, 2061.
33. Rees, M. J., *Class. Quant. Grav*., 1997, **14**, 1411.
34. Komossa, S. *et al*., *Astrophys. J.*, 2003, **582**, L15–L20.
35. Merritt, D. and Ekers, R. D., *Science*, 2002, **297**, 1310–1313.
36. Haehnelt, M. G., In *Laser Interferometer Space Antenna* (ed. Folkner, W. M.), AIP, Woodbury, NY, 1998.
37. Sathyaprakash, B. S., Problem of searching for spinning black hole binaries, Proceedings of the XXXVIII Recontres, de Moriond, 24–29 March 2003 (in press).
38. Sathyaprakash, B. S. and Schutz, B. F., *Class. Quant. Grav*., 2003, **20**, S209.
39. Ryan, F. D., *Phys. Rev. D.*, 1995, **52**, 5707.
40. Phinney, S., 2001, private communication.
41. Müller, E., In *Relativistic Gravitation and Gravitational Radiation* (eds Lasota, J.-P. and Marck, J.-A.), Cambridge Univ., Cambridge, 1997.
42. Andersson, N. and Kokkotas, K., *Int. J. Mod. Phys*., 2001, **10**, 381.
43. Chandrasekhar, S., *Phys. Rev. Lett.*, 1970, **24**, 611.
44. Friedman, J. L. and Schutz, B. F., *Astrophys. J.*, 1978, **222**, 281.
45. Andersson, N., *Astrophys. J.*, 1998, **502**, 708.
46. Lindblom, L., Owen, B. J. and Morsink, S. M., *Phys. Rev. Lett.*, 1998, **80**, 4843.
47. Andersson, N., Jones, D. I. and Kokkotas, K., *Mon. Not. R. Astron. Soc.*, 2001, **337**, 1224.
48. Bildsten, L., *Astrophys. J. Lett.*, 1998, **501**, 89.
49. Cutler, C., *Phys. Rev. D*., 2002, **66**, 084025.
50. Thorne, K. S., Gravitational radiation. In *300 Years of Gravitation* (eds Hawking, S. W. and Isreal, W.), Cambridge University Press, Cambridge, 1987, p. 330.
51. Allen, B. and Romano, J. D., *Phys. Rev. D.*, 1999, **59**, 102001.
52. Hils, D., Bender, P. L. and Webbink, R. F., *Astrophys. J*, 1990, **360**, 75.